PROCEEDINGS B

royalsocietypublishing.org/journal/rspb

Research

Cite this article: Rauscher MJ, Fox JL. 2024 Asynchronous haltere input drives specific wing and head movements in *Drosophila*. *Proc. R. Soc. B* **291**: 20240311.
https://doi.org/10.1098/rspb.2024.0311

Received: 29 June 2023
Accepted: 19 April 2024

Subject Category:
Behaviour

Subject Areas:
behaviour

Keywords:
animal behaviour, *Drosophila*, haltere, insect flight, wing hitch, multisensory integration

Author for correspondence:
Jessica L. Fox
e-mail: jlf88@case.edu

Electronic supplementary material is available online at https://doi.org/10.6084/m9.figshare.c.7204039.

THE ROYAL SOCIETY PUBLISHING

Asynchronous haltere input drives specific wing and head movements in *Drosophila*

Michael J. Rauscher and Jessica L. Fox

Department of Biology, Case Western Reserve University, Cleveland, OH, USA

MJR, 0000-0002-0607-1083; JLF, 0000-0001-6374-657X

Halteres are multifunctional mechanosensory organs unique to the true flies (Diptera). A set of reduced hindwings, the halteres beat at the same frequency as the lift-generating forewings and sense inertial forces via mechanosensory campaniform sensilla. Though haltere ablation makes stable flight impossible, the specific role of wing-synchronous input has not been established. Using small iron filings attached to the halteres of tethered flies and an alternating electromagnetic field, we experimentally decoupled the wings and halteres of flying *Drosophila* and observed the resulting changes in wingbeat amplitude and head orientation. We find that asynchronous haltere input results in fast amplitude changes in the wing (hitches), but does not appreciably move the head. In multimodal experiments, we find that wing and gaze optomotor responses are disrupted differently by asynchronous input. These effects of wing-asynchronous haltere input suggest that specific sensory information is necessary for maintaining wing amplitude stability and adaptive gaze control.

1. Introduction

Animal locomotion, from crawling [1] to swimming [2] to walking [3] to flight [4], typically requires coordinated motion of multiple body segments or appendages. Though this coordination can stem from activity in a central pattern generator, proprioceptive input modulates body motions to adapt each step [5,6]. Specific contraction timing of muscles actuating multiple appendages can significantly change gait, and thus the mechanisms ensuring limb coordination are essential to structuring adaptive locomotion.

In flying flies, wing [7] and haltere [8] proprioceptors provide crucial feedback allowing for active control of each wingstroke to counteract flies' inherent pitch instability [9]. The halteres are small club-shaped organs which have evolved from hindwings in true flies (Diptera). Long known to be required for stable flight [10], the halteres do not generate significant lift, but instead primarily detect inertial forces using campaniform sensilla at their base [8,11,12]. Afferent neurons from haltere campaniform sensilla entrain their firing to a preferred phase of the haltere stroke cycle [13,14], which in *Drosophila* and most other fly taxa is biomechanically linked to the wing stroke cycle with an antiphase synchrony [15,16].

Stroke-synchronous feedback from halteres is functionally important for wing-steering motoneurons and muscles [8,17,18]. In tethered flight, haltere ablation results in variable wing amplitudes and diminished wing optomotor responses [19–21]. In the blowfly *Calliphora*, some haltere afferents project directly to the motoneuron controlling wing-steering muscle wB1 [22]. Stimulation of the haltere nerve can entrain firing of the motoneuron, which is normally more sensitive to wing reafference, if it occurs within a specified time relative to the wing nerve's firing [23]. Optogenetic activation of haltere muscles resets the firing phase of both the wB1 and wB2 muscles [18]. For these reasons, we hypothesized that asynchronous haltere input is insufficient

for stable wing muscle output, and predicted that changing the phase of the haltere's stroke would cause wing amplitude instabilities distinct from those observed in ablation experiments.

Haltere amplitude manipulation results in smooth changes in wingstroke amplitude and gaze direction [24]. However, flies often execute sharp changes in wingstroke amplitude that can take on a variety of time courses. Fast, unilateral 'wing hitches' can occur spontaneously [25,26]. These contrast with longer saccades [27,28], which can be either spontaneous or driven by visual input [29–32] and involve coordinated syndirectional motion of both wings and the head [33–36]. Both saccades and wing hitches are distinct outputs of wing and neck motor pathways, and observing how sensory modulation influences them can reveal pathways for processing sensory input.

Neck motoneurons also receive input from haltere afferents [37,38], and mediate a similar suite of gaze-stabilizing reflexes [39]. However, the mechanisms by which the neck motoneurons integrate multisensory information to drive the head are not fully characterized. Flies without halteres lose the ability to modulate the gain of optomotor responses [40], but flies with decreased haltere amplitude do not [24]. In some neck motoneurons, spiking responses to visual input are gated, but not modified, by haltere input [41]. This evidence suggests that general haltere excitation may be necessary for optomotor responses, but that the specific haltere motion may have little influence. We thus hypothesized that stroke-synchronous haltere information is not strictly necessary for visually guided head movements. Alternatively, modulation by other senses and/or behavioural state may influence haltere effects on gaze control: flies receiving haltere input from self-generated body rotations have distinct head movements from those experiencing passive rotations from a servo motor [36], despite identical body motions.

To examine how halteres drive wing and gaze behaviours, we experimentally decoupled wing and haltere movement with both static and dynamic perturbations. By adding a small iron mass to one haltere, we immobilized it, abolishing it as a source of mechanosensory information. Then, using electromagnets, we drove the haltere at specific frequencies, moving it throughout its natural range of motion asynchronously with the wings. An asynchronously driven haltere increased the likelihood of unilateral wing hitches, but this did not occur in movements of the head. Optomotor responses of both head and wings were significantly diminished. Our results show that asynchronous haltere input is insufficient for wing amplitude stabilization and optomotor responses, and results in head responses of diminished amplitude.

2. Material and methods

(a) Animal care, haltere manipulations and experimental trials

Animals were reared from a colony of wild-caught *Drosophila melanogaster*. Female flies (3–5 days post-eclosion) were cold-anaesthetized and attached to tungsten pins using UV-curing cement. For magnetic stimulation experiments, a single iron filing was attached to the right haltere with UV-curing cement. Only iron filings of sufficient mass to immobilize the haltere (in excess of ~12 µg, [24]) were used for experiments. For ablation experiments, one or both halteres were completely removed using fine forceps. For filing-treated animals, successive presentations of different haltere stimuli were preceded and followed by control epochs with the magnets disengaged lasting a minimum of 250 ms. For each animal, 1–6 epochs from the same experimental condition were drawn for analysis.

(b) Haltere stimulation

To control haltere kinematics, two iron-core electromagnets were positioned anterior-dorsal and posterior-ventral to the fly (figure 1; [24]). Each electromagnet was powered from a variable power supply (TP1803D, Tekpower, Montclair, CA, USA) switched through a power transistor (D1276A, Panasonic, Kadoma, Japan) and controlled via 5V TTL-level output from a data acquisition board (USB-6434, National Instruments, Austin, TX, USA). Pulse trains consisted of 50% duty cycle square wave signals alternating at 25, 36, 50, 72, 100 or 167 Hz. Signals to the magnets were 180° out of phase to produce a dorsal–ventral oscillation at the commanded frequency.

(c) Visual stimulation

To elicit optomotor responses, we used a wide-field vertical stripe pattern moving in the yaw aspect under the control of a 1 Hz triangle wave, presented using a modular light-emitting diode (LED) flight arena [42]. Stripes were one or two pixels wide and pseudo-randomly spaced such that average luminance of the wide-field panorama was 50% [43]. Different pattern velocities were achieved by varying the amplitude of the triangle wave while keeping the period constant.

(d) High-speed video and kinematic measurements

Haltere and wing kinematics were recorded using two synchronized high-speed cameras (TS4 or IL5, Fastec Imaging, San Diego, CA, USA) with sagittal views of the fly from the left and right. Recordings were made at 1000 or 2000 fps for all treated animals and the majority of untreated animals; some untreated animals were recorded at 750 fps. In each video, the haltere bulb was digitized using the DLTdv8 [44] or DeepLabCut [45] software packages. Wingbeat elevation time series were extracted using a custom MATLAB script. A third camera recording at 100 fps (Point Grey Chameleon3, FLIR, Wilsonville, OR, USA)

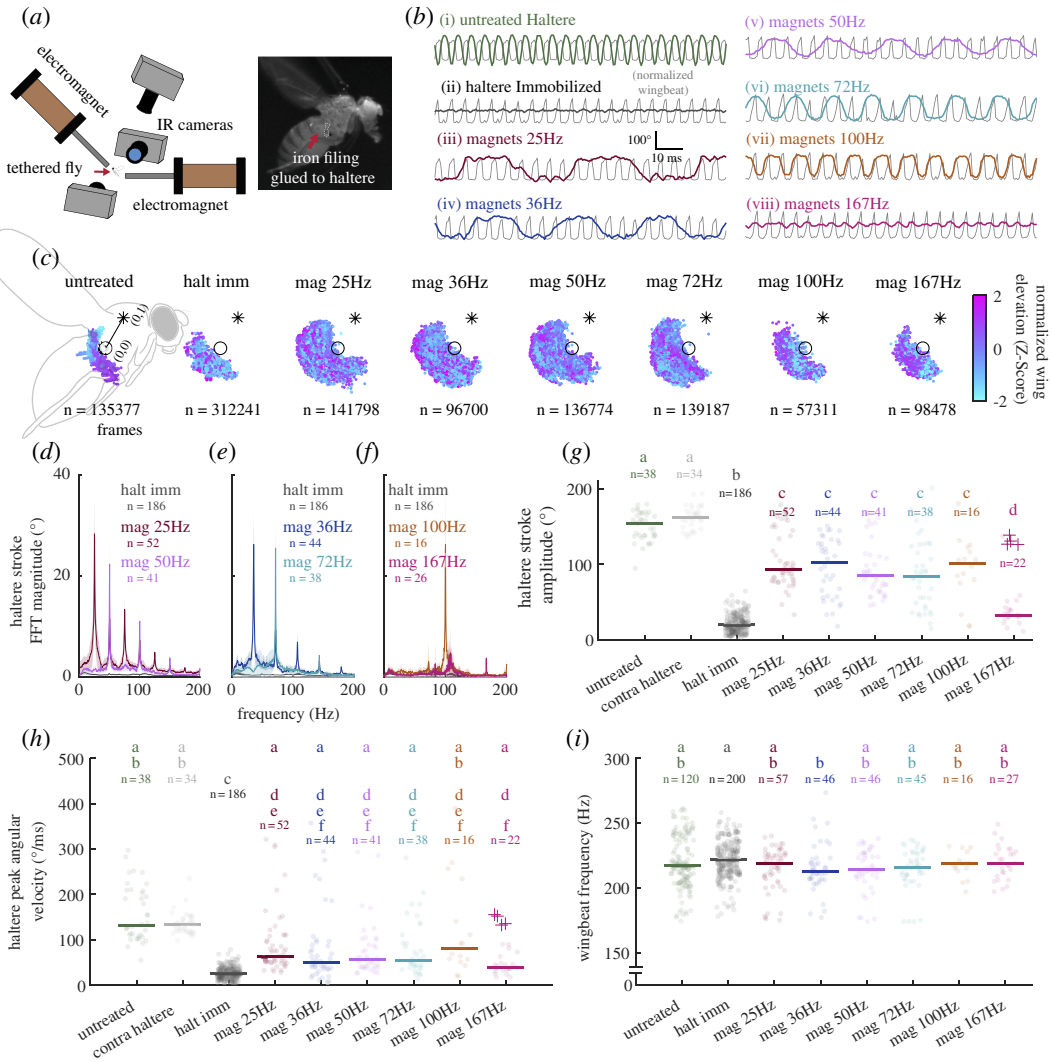

Figure 1. Electromagnetic control of haltere movement asynchronous from the wings. (*a*) Schematic of iron filing treatment (top, inset) and electromagnetic stimulation system (bottom). (*b*) Representative traces showing movement of untreated haltere at wingbeat frequency (i), immobilized haltere treated with iron filing (ii), and actively driven haltere at a range of frequencies (iii–viii) controlled by electromagnets. (*c*) Haltere tracking by condition, registered into a normalized body coordinate system defining the haltere base as the origin, represented by a circle and the anterior wing base as (0,1), represented by an asterisk. Colours reflect the Z-normalized wing stroke elevation at each measurement point. (*d*) Mean FFT (95% confidence interval shaded) of all high-speed (1000 or 2000 fps) time series with the haltere immobilized (black), driven at 25 Hz (red) and 50 Hz (pink). (*e*) same as (*d*) for 36 Hz (blue) and 72 Hz (teal) frequencies. (*f*) same as (*d*) and (*e*) for 100 Hz (orange) and 167 Hz (magenta) frequencies. (*g–i*) Haltere stroke amplitude (*g*), peak angular velocity (*h*) and baseline wingbeat frequencies (*i*) observed under each haltere manipulation. Lines show median for each group. 167 Hz responses from outlier animal shown with +. Letters denote statistical groupings from multiple Bonferroni-corrected Wilcoxon rank-sum tests (5% alpha).

provided a dorsal view to measure head and wing kinematics. Head yaw and wing downstroke envelope kinematic time series were computed using a custom MATLAB program called Flyalyzer (https://github.com/michaelrauscher/flyalyzer; [24]).

(e) Wing hitch detection and analysis

Wing hitches (described in figures 2–4) were identified from baseline-subtracted video segments using a custom MATLAB script utilizing the built-in peak detection function, selecting peaks with a minimum amplitude of 4° (after the saccade detection algorithm in [34]). To capture hitches as described by Götz [25,26] while excluding saccades, we screened putative hitches for a maximum duration of 40 ms and a minimum prominence of 4°. Here, prominence refers to the height of the peak versus an adaptive reference level dependent upon neighbouring peaks, following an algorithm described in the peak-detection function reference. All detected hitches were used to calculate the hitch rates shown in figure 2*c,d*, figure 4*c,d* and electronic supplementary material, figure S2*d–i*. For the event-triggered average (ETA) responses shown in figure 2*e–h* (and electronic supplementary material, figure S2*a–e*) as well as the cyclic average responses shown in electronic supplementary material, figure S3, hitches were included only from video segments with concurrent high-speed haltere and wing tracking from the lateral aspect cameras. Each 80 ms event-triggered window used to produce the ETA was baseline-subtracted and matched to a control window selected with a randomly drawn frame index from the same video segment. To produce the histograms shown in figure 3*b–g* and the heatmaps shown in electronic supplementary material, figure S4, data were pooled from all available asynchronously driven stimulus categories (up to and including 167 Hz). Each frame from the 100 fps camera was assigned a haltere position and wing instantaneous phase value at frame start by finding the single nearest-match frame recorded on the

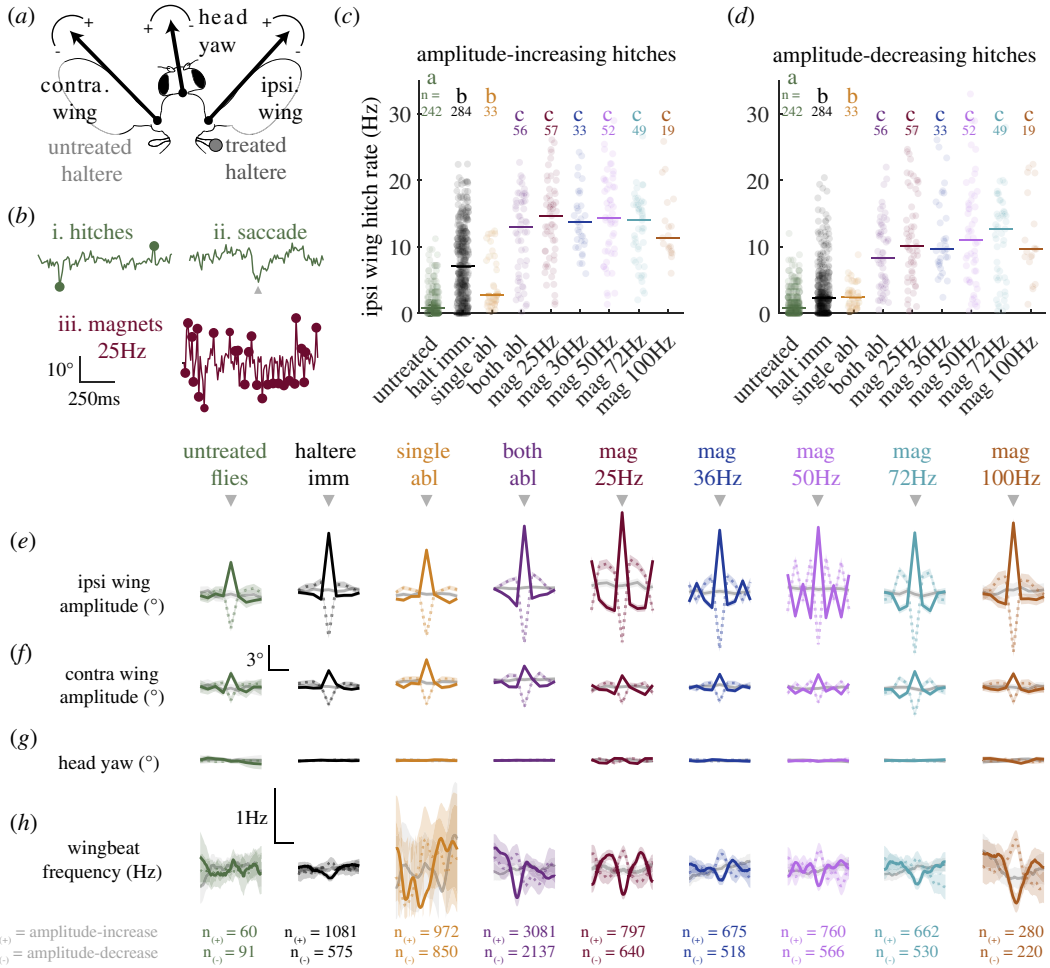

Figure 2. Haltere manipulation increases ipsilateral wing hitch rate. (*a*) Schematic of measured kinematic outputs, recorded at 100 fps, showing downstroke amplitude (angle of wing envelope leading edge) for each wing and yaw movement of the head. Arcs denote the sign (positive or negative) of clockwise and anticlockwise rotations for each parameter. (*b*) Example of ipsilateral wing amplitude traces showing fast wing hitches from untreated animal (i), similar in amplitude but distinct in temporal dynamics from a wing saccade (ii) and increased hitch rate observed in an animal with an asynchronously driven haltere (iii). Hitches are annotated with filled circles. Saccade with a grey triangle. (*c*) Rate of all ipsilateral wing hitches of increasing amplitude across all haltere treatments (see §2). Left and right wing responses for symmetrical manipulations (untreated, bilateral ablation) are pooled. Lines show median for each group. Letters denote statistical groupings from multiple Bonferroni-corrected Wilcoxon rank-sum tests (5% alpha). (*d*) Same as (*c*) but for amplitude-decreasing hitches. (*e*) Event-triggered average (ETA) responses for each condition, generated from time-aligned, baseline-subtracted kinematic timeseries. Grey triangles show the hitch peak, around which each constitutive video segment of the ETA is indexed, with amplitude-increasing hitch ETAs shown with solid lines and amplitude-decreasing hitch ETAs shown with dashed lines (shade, 95% confidence interval). Grey traces show controls triggered from random indices within the same time series. (*f–h*) Same as (*e*) but for concurrent movements of the contralateral wing (*f*), head yaw (*g*) and baseline-subtracted instantaneous wingbeat frequency (*h*).

high-speed lateral aspect cameras (1000 or 2000 fps). To assign a single angular velocity value to each frame from the 100 fps camera, the root-mean-square value of the angular velocity time series was computed for all concurrent frames from the lateral aspect camera. Then, the sign (positive or negative) of the lateral aspect frame with the largest absolute value was applied to the result. A graphical summary of this process is included in electronic supplementary material, figure S4*a*.

(f) Frequency-domain analysis

For estimation of visual response magnitude (figure 5), kinematic time series were offset-levelled by fitting a least-squares regression line and then subtracting it out to remove linear trends, then zero-padded to 4096 samples. Magnitude estimates from resultant FFTs were then divided by the number of samples in each time series prior to zero-padding to normalize magnitudes for trials of varying length. Only segments longer than 64 samples were used, resulting in a coarsest possible spectral resolution of 1.5 Hz.

3. Results

(a) Electromagnetic control of haltere stroke kinematics

To establish magnetic control over one haltere, an iron filing was attached to the bulb (figure 1*a*). With the electromagnets deactivated, this mass immobilized the haltere and prevented the fly from oscillating it. Activation of the electromagnets

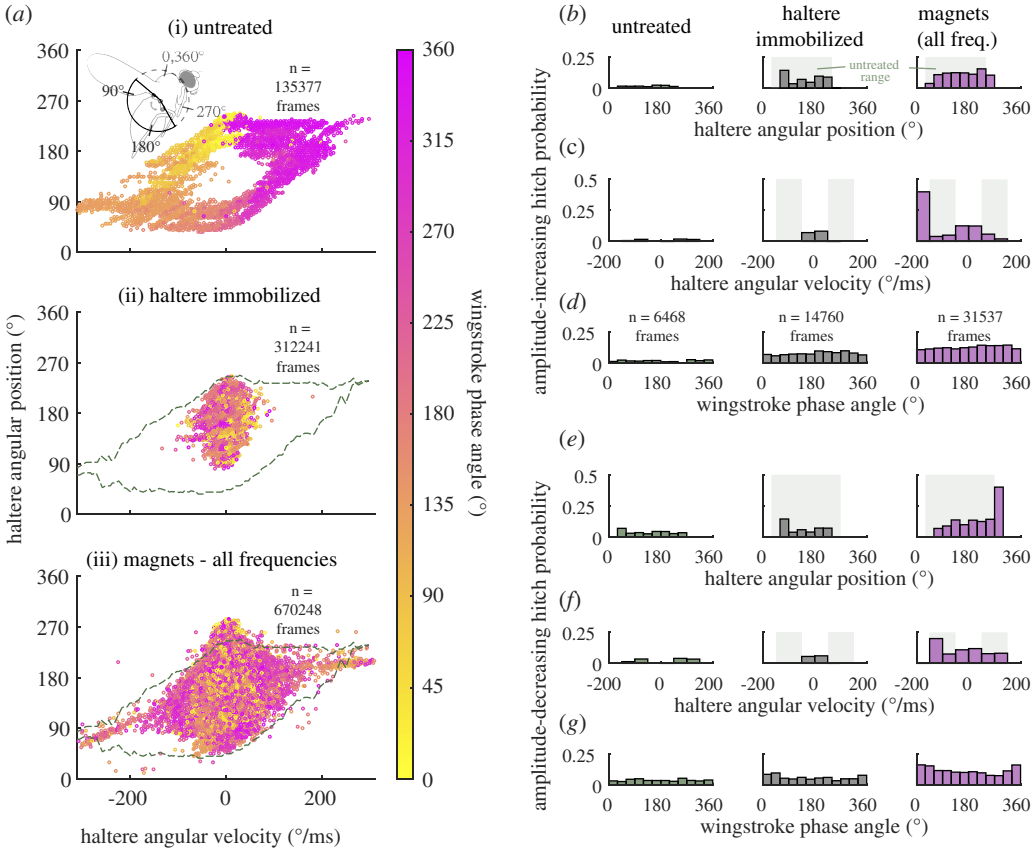

Figure 3. Ipsilateral wing hitches are more likely when the haltere exceeds normal kinematic parameters. (*a*) Summary of haltere angular position, angular velocity and wing instantaneous phase from all high-speed data, separated by condition. (*a*(i)) Untreated animals, showing natural antiphase synchrony of haltere and wings. Inset shows the unified body coordinate scheme, with haltere upstrokes typically occupying the 45–90° range and downstrokes typically occupying the 235–270° range. (*a*(ii)) Frames from haltere immobilized (magnets OFF) condition. Green dashed line shows the extent of the naturalistic parameter space observed in the untreated animal. (*a*(iii)) High-speed frames aggregated from all magnetic stimulation frequencies, showing broad overlap with the naturalistic range of haltere angular velocities and angular positions. (*b*) Histograms of ipsilateral wing amplitude video frames showing probability of amplitude-increasing hitch as a function of haltere angular position at frame onset for each condition. Light green shaded region outlines the natural range of haltere angular positions. (*c*) Same as (*b*) but for haltere signed-RMS angular velocity throughout the frame (see §2). Light green shaded regions outline the naturalistic range of negative (upstroke) and positive (downstroke) angular velocities. (*d*) Same as (*b*) but for wing instantaneous phase at frame onset. (*e–g*) Same as (*b–d*) but for amplitude-decreasing hitches.

at 25, 36, 50, 72, 100 and 167 Hz resulted in movement of the haltere at the commanded frequency (figure 1*b–f*, electronic supplementary material, video S1). This method resulted in haltere movement both within and outside of its naturalistic range (figure 1*c*), with all possible phase relationships to the wing. In all the observed trials, the untreated haltere maintained full stroke amplitude (figure 1*g*). At the highest frequency tested (167 Hz), 13 out of 14 flies were unable to maintain a haltere amplitude that was within the range of those observed naturally (figure 1*g*, 22 of 27 replicate trials). We thus excluded 167 Hz trials from further analyses that compared across conditions (see §2). All conditions achieved peak angular velocities within the range of those observed in untreated animals (figure 1*h*). Wingbeat frequencies were statistically indistinguishable from untreated controls for all treatments (figure 1*i*), showing that manipulations did not impair the gross functioning of the wing motor system.

(b) Asynchronous haltere movement increases wing hitch rate

Haltere-manipulated flies showed significantly higher rates of wing hitches than untreated control animals, for hitches reflecting wing amplitude increase as well as for hitches of decreasing amplitude (figure 2*a–d*, electronic supplementary material, video S2). All treatments exhibited higher rates of ipsilateral wing hitches than untreated controls. For both amplitude-increasing hitches (figure 2*c*) as well as amplitude-decreasing hitches (figure 2*d*), dynamic haltere stimulation at any frequency resulted in ipsilateral wing hitch rates comparable to those seen with bilateral haltere ablation, whereas haltere immobilization resulted in intermediate hitch rates comparable to those seen with unilateral ablation.

Saccades are accompanied by coordinated movement of the contralateral wing and head. Examining the responses of the contralateral wing and head immediately following an ipsilateral hitch (event-triggered averages; figure 2*e–h*), we found that this was not true of wing hitches. Under every condition, each ipsilateral wing hitch (figure 2*e*, electronic supplementary material, figure S2*a*) was accompanied by very small changes in the amplitude of the contralateral wing (figure 2*f*, electronic supplementary material, figure S2*b*) and no meaningful change in head yaw (figure 2*g*, electronic supplementary material, figure S2*c*). The small changes in contralateral stroke amplitude very rarely met identification criteria for a wing hitch (electronic supplementary material, figure S2*d–e*). While all treatment groups did exhibit higher rates of contralateral hitches than

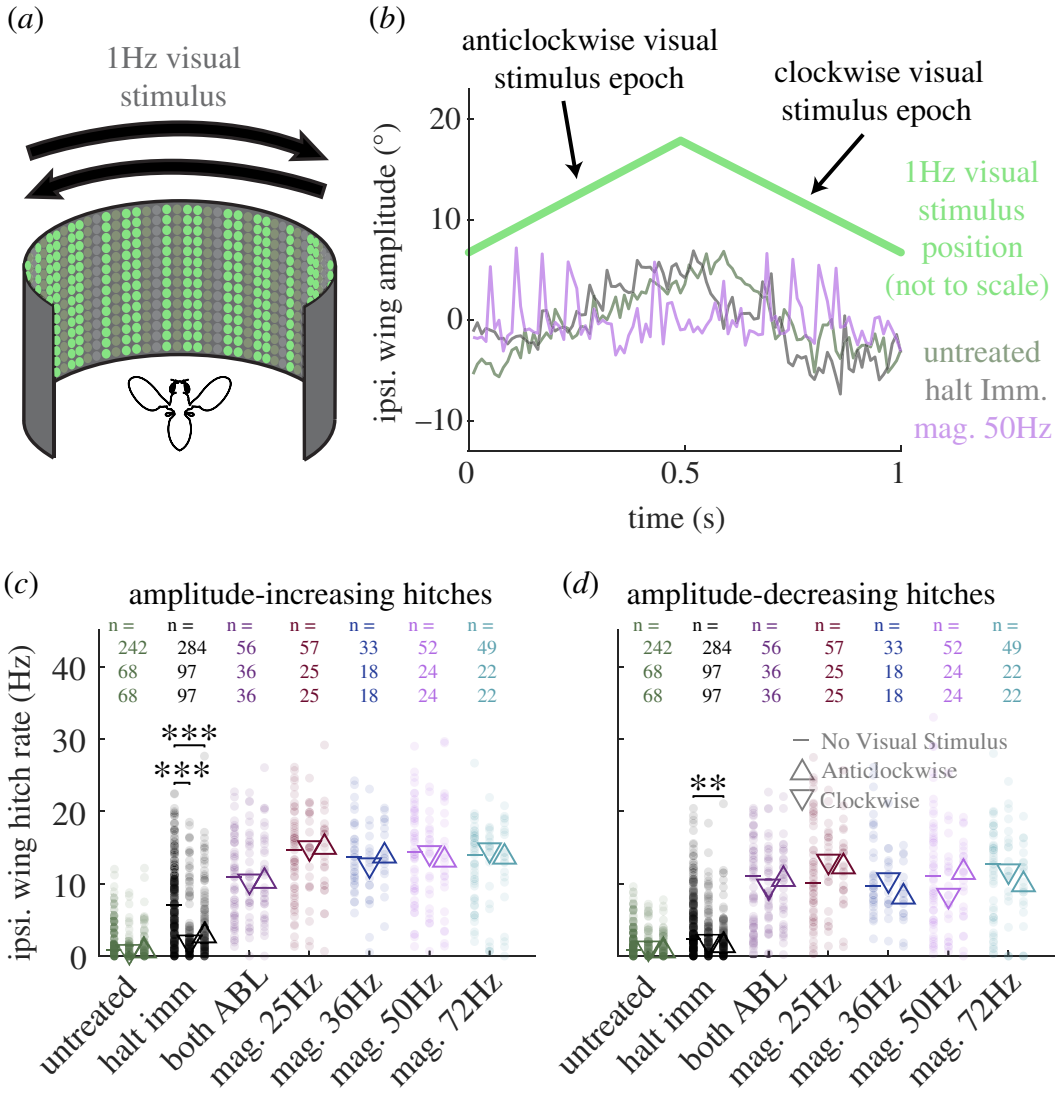

Figure 4. Concurrent visual input does not influence wing hitch rate during most haltere manipulations. (*a*) Schematic of visual stimulus, showing irregular stripe pattern moving on an LED panel under the control of a 1 Hz triangle-wave with a pattern velocity of 90°/s. (*b*) Example of ipsilateral wing amplitude responses to one cycle of the visual stimulus under several haltere treatment conditions. (*c*) Rate of increasing-amplitude ipsilateral wing hitches across visual conditions, showing no change between uniform visual stimulus (reproduced from figure 2), clockwise visual stimulus epochs and anticlockwise epochs in most haltere treatment conditions. Mean value for each visual stimulus condition represented by a dash, upward pointing triangle and downward pointing triangle, respectively. (*d*) Same as (*c*) but for amplitude-decreasing ipsilateral wing hitch rate (** = significance at 1% alpha level, *** = significance at 0.1% alpha level, multiple Bonferroni-corrected Wilcoxon rank-sum tests).

untreated controls, these hitches were not coordinated with the ipsilateral hitches. Accordingly, the rate of head yaw deviations of equivalent magnitude to a wing hitch was virtually zero under all treatment conditions (electronic supplementary material, figure S2*h–i*). Wing and head kinematics during wing hitches did not resemble the coordinated syndirectional movement of the head and wings seen in saccades, emphasizing that these two behaviours are categorically different.

(c) Haltere kinematic parameters influence hitch initiation

If haltere manipulations directly drive hitches, the hitch rate should increase with increasing stimulus rate. However, wing hitch rate was uniform across stimulation frequencies, and indistinguishable from that seen with bilateral haltere ablation. Despite this, ETAs of the ipsilateral wing amplitude (figure 2*e*) and wing instantaneous frequency (figure 2*h*) oscillated in time with the driving stimulus. Also, fast Fourier transforms (FFTs) of wing and head kinematic time series (electronic supplementary material, figure S1) showed elevated power at the magnetic stimulation frequency (or its baseband alias, for frequencies which exceeded the Nyquist limit of the kinematics camera). Similarly, stimulus-triggered cyclic averages aligned on each magnetic stimulation pulse showed that hitch probability varied in time with the stimulus for both amplitude-increasing and amplitude-decreasing wing hitches (electronic supplementary material, figure S3a). Taken together, these data suggest that hitches occurred at specific times relative to the driving stimulus but were not elicited upon every stroke cycle.

Cyclic averages also illustrated that whereas the treated haltere's frequency and amplitude were reliably commanded with the electromagnets, the oscillation assumed a diversity of phase relationships with the stimulus across animals and between trials (electronic supplementary material, figure S3*b–d*). This technical limitation implies that stimulus timing

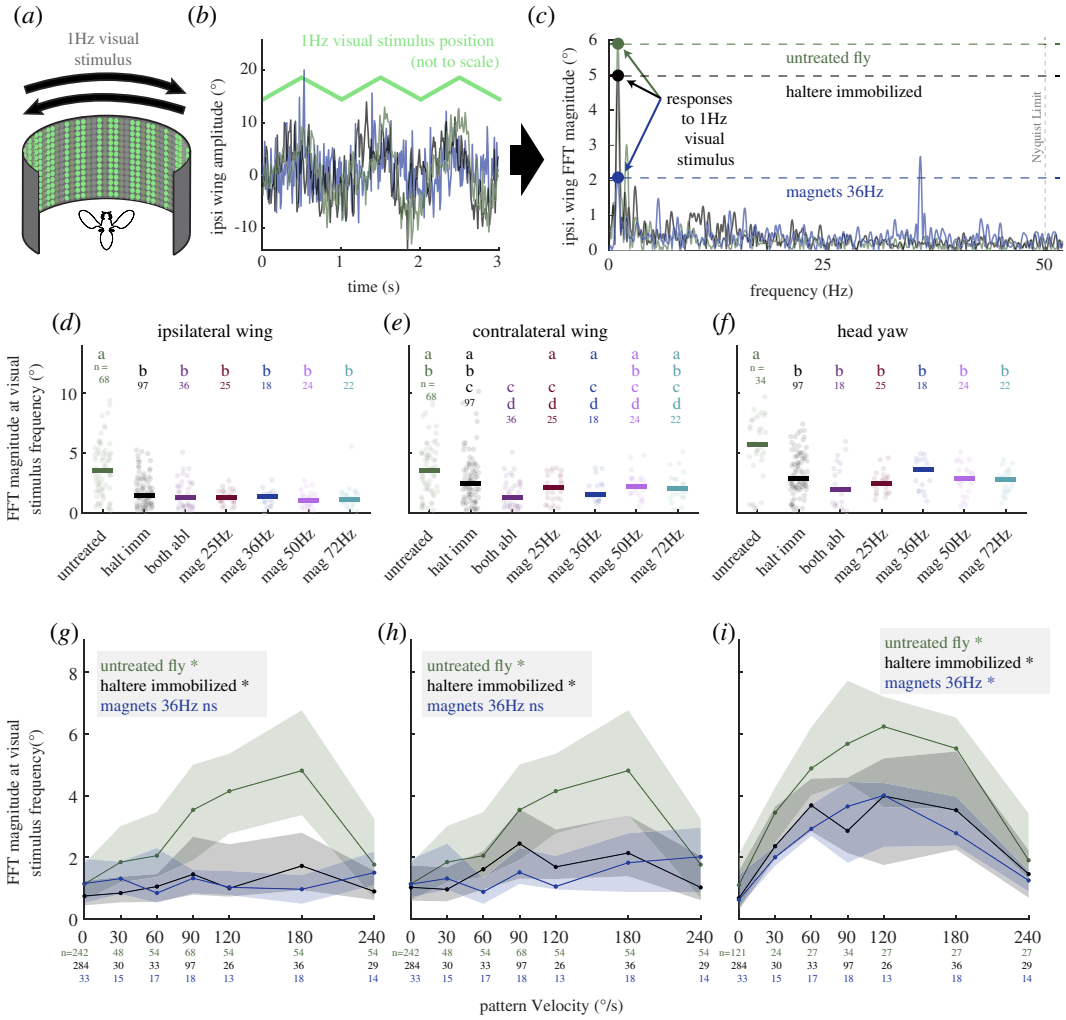

Figure 5. Haltere manipulations influence visually guided wing and head movements. (*a*) Schematic of visual stimulus, as in figure 4*a*. (*b*) Example of ipsilateral wing amplitude responses to multiple cycles of the visual stimulus under several haltere treatment conditions. (*c*) FFTs of traces from (*b*), showing peak at the frequency of the visual stimulus. (*d*) Ipsilateral wing response amplitude at visual stimulus frequency for all tested haltere treatments. For symmetrical manipulations (untreated, bilateral ablation), left and right wing responses are pooled. Letters denote statistical groupings from multiple Bonferroni-corrected Wilcoxon rank-sum tests (5% alpha). (*e*,*f*) Same as (*d*) for contralateral wing and head yaw responses, respectively. Lines show median for each group. (*g*) Ipsilateral wing visual response magnitude, as estimated by measuring the FFT magnitude at visual stimulus frequency, for untreated flies, haltere-immobilized flies and 36 Hz magnetic stimulation flies. Trendlines connect median data from each pattern velocity, with shaded regions showing first and third quartiles. Inset, results of Kruskal–Wallis omnibus test indicate whether pattern velocity is a significant predictor of response amplitude within each treatment group at the 5% alpha level (*) or not (ns). (*h*–*i*) Same as (*g*), but for contralateral wing and head yaw amplitude, respectively.

could not necessarily predict specific haltere positions or phases: these had to be measured directly from high-speed video.

After observing phase-locked wing hitches, we examined whether specific haltere kinematic parameters drove hitch initiation. We assessed the haltere's angular position, angular velocity and phase relationship to the wingstroke cycle (figure 3*a*). We found that our manipulations resulted in values both within and outside of the range of values observed in untreated animals, allowing us to observe responses to both naturally occurring stimuli and stimuli that do not occur in flight.

We then created histograms assessing the probability of hitch initiation as a function of each kinematic parameter under each condition, performing separate analyses for amplitude-increasing (figure 3*b–d*) and amplitude-decreasing hitches (figure 3*e–g*). Amplitude-increasing hitch probability was not related to haltere angular position under any condition (figure 3*b*), however, amplitude-decreasing hitches were comparatively more likely for the dynamically stimulated conditions when the haltere was in a downstroke position that exceeded its naturalistic stroke limits (figure 3*e*, right). In untreated animals, the haltere's angular velocity was almost always high, whether the haltere was moving up or down (figure 3*c*, grey bars); in haltere-immobilized animals, the angular velocity was always low. Hitch probability was also low in these static conditions, although higher in immobilized animals. When we dynamically perturbed the haltere in a velocity range either faster or slower than its natural activity, however, we saw a dramatic increase in amplitude-increasing hitch probability (figure 3*c*, right). For both amplitude-increasing and amplitude-decreasing hitches, there was no relationship between wing phase and hitch probability under any condition (figure 3*d*,*g*). Multivariate probability heatmaps of multiple kinematic parameters did not reveal any trends over and above those outlined in univariate analysis (electronic supplementary material, figure S4). Our data, therefore, show that flies respond to unnatural haltere velocities by initiating ipsilateral wing hitches, with little discernable influence from other measured kinematic parameters.

(d) Haltere-evoked hitches are not influenced by concurrent visual stimulation

The fly thoracic nervous system integrates inertial sensory information from the halteres with information from the fly's visual system [38,46,47]. Tethered flies adjust gaze and wingstroke amplitude in response to visual movement [39,48] using a motor pool shared with reflexes driven by the halteres [36,49]. Could visual input influence wing hitches evoked by haltere stimulation?

Concurrently with each haltere treatment, we presented a wide-field pattern of high-contrast vertical stripes with a pattern velocity of 90°/s (figure 4*a*,*b*, electronic supplementary material, video S3). We then subdivided each stimulus epoch into periods of clockwise and anticlockwise visual motion (figure 4*a*,*b*) and calculated hitch rate during each period (as in figure 2). In both visual stimulus directions and for both amplitude-increasing and amplitude-decreasing hitches, visual stimulation did not affect hitch rate under most haltere stimulus conditions (figure 4*c*,*d*). Notably, however, concurrent visual stimulation in either direction reduced the rate of amplitude-increasing ipsilateral hitches when the haltere was immobilized (figure 4*c*). For amplitude-decreasing hitches, this was observed only for stimulation in the anticlockwise direction (figure 4*d*). Similar results were observed for the contralateral wing (electronic supplementary material, figure S5). Our results suggest that descending visual input cannot 'rescue' the wing from the effects of asynchronous haltere input.

(e) Asynchronous haltere movement disrupts wing and head optomotor responses

Halteres adjust the gain of wing and gaze optomotor equilibrium reflexes [20,21,36,40,50]. Is asynchronous input sufficient to drive these? We estimated the optomotor response amplitude (following [50]) by measuring the magnitude of the FFT of each kinematic time series at 1 Hz, the frequency of the visual stimulus (figure 5*a*–*c*). For the ipsilateral wing and head (figure 5*d*,*f*), all haltere manipulations resulted in smaller visual response amplitudes than those of untreated flies. For the contralateral wing, only the bilateral ablation was statistically distinct (figure 5*e*).

Static haltere manipulations (bilateral ablation and immobilization) impair the ability of flies to adjust their head responses to widefield visual stimuli, locking the fly into a fixed low-amplitude response to all salient pattern velocities [40]. We presented a subset of flies with a series of visual stimuli that moved at a range of pattern velocities, 30–240°/s. Untreated flies exhibited an optomotor tuning curve that peaked at 180°/s for wing responses (figure 5*g*–*h*, electronic supplementary material, figure S6*a*,*b*) and 120°/s for head responses (figure 5*i*, electronic supplementary material, figure S6*c*), in agreement with previous studies [40,48]. Similar tuning curves were observed for flies with immobilized halteres (figure 5*g*–*i*) although with significantly lower response amplitudes than untreated flies (electronic supplementary material, figure S6*d*–*f*). Under dynamic stimulation (magnets engaged at 36 Hz), optomotor tuning was abolished for both contralateral and ipsilateral wings. Visual pattern velocity was not a significant predictor of response amplitude for these flies (figure 5*g*–*h*). In comparison, head responses showed lower gain relative to untreated controls, at levels comparable to those seen with haltere immobilization (figure 5*i*, electronic supplementary material, figure S6*c*,*f*).

4. Discussion

For locomotion, coordinated appendages are so important that it is often difficult to force uncoordinated movement: in flying flies, passive thoracic biomechanics restrict halteres and wings to oscillate in antiphase [16]. We used stimuli both within and outside the bounds of natural haltere motions to demonstrate that wing steering reflexes are critically impaired by asynchronous haltere input, with increased ipsilateral wing hitches following 'unnatural' haltere movements (figures 2 and 3). In doing so, we showed that asynchronous haltere input is uniquely deleterious to ipsilateral wing control.

Though we hypothesized that any haltere input would be sufficient for full-amplitude visually guided head movements, we instead observed that asynchronous haltere input results in lower amplitude movements (figure 5). The head's movements, though driven by a more diverse set of inputs and occurring at lower speeds, still show deleterious effects of asynchronous haltere input. Asynchronous haltere input did not evoke head yaw changes comparable to those seen in the wing (figure 2), congruent with previous findings that abrupt changes in head yaw (as part of a saccade) are primarily evoked by proprioceptive inputs [34]. We show that dynamic haltere perturbations drive 'wing hitches', short-duration changes in amplitude that can occur unilaterally. These hitches may be a component of the body saccade, a coordinated movement of the head and both wings which is used to reorient the flying fly.

(a) Asynchronous haltere input increases wing hitches

Asynchronous dynamic haltere input increases the rate of ipsilateral wing hitches (figure 2), particularly when the haltere moves at angular velocities outside of its natural operating range. The halteres are sensitive to the body's angular velocity [19]; here, we show that they are sensitive to their own angular velocity as well (figure 3). Our experiment with one immobilized haltere shows that hitches are not driven by specific motions of the haltere: loss of one or both halteres also results in an elevated rate of hitches of similar amplitude. Therefore, another possible interpretation is that hitches emerge spontaneously from activity of the wing motor system, and that synchronous haltere input acts to suppress them.

Campaniform sensilla are sensitive to compressive and shearing forces [8,51,52], which arise from the haltere's movement and scale with the bulb's angular velocity [53]. We might therefore predict that hitches are more or less likely to be initiated

as a function of the haltere's angular position. Our results suggest that amplitude-decreasing hitches are more likely when the haltere is hyperextended past its natural downstroke position, we did not otherwise observe a strong correspondence between haltere angular position and hitch initiation (figure 3). This suggests, but does not conclusively show, that the halteres suppress spontaneous hitches rather than driving hitches at specific positions. The extreme sensitivity of the sensilla [14,54] requires us to consider the possibility that we were not able to stimulate accurately enough to reach this conclusion. The overall effect on flight behaviour is the same under both hypotheses: the halteres have a stabilizing effect on wing amplitude and thus on body rotations, reflecting prior experimental and theoretical work [4,55,56].

(b) Coordinated movement and haltere influence on the contralateral wing

In our previous work [24], manipulating haltere stroke amplitude without compromising haltere-wing synchrony evoked a smooth wing-steering response. Here, responses to haltere perturbation were less stereotyped, but in neither the present nor the previous work was there a clear relationship between instantaneous wing phase and haltere-evoked changes in wing kinematic parameters (figure 3). This was surprising given the organization of the wing-steering motor system, a major component of which are tonic muscles which fire once every stroke cycle and control muscle tension by varying the firing phase within it [57–60]. While our stimulation sampled the entire range of wing/haltere phases, a limitation of our experimental paradigm is that we could not stimulate with a particular phase combination for consecutive stroke cycles, which may be important for the force production properties of these muscles. Another hypothesis is that the untreated contralateral haltere provides enough input to supersede an absent or malfunctioning ipsilateral haltere.

Our findings that asynchronous haltere input increases the rate of contralateral wing hitches independent of movements accompanying ipsilateral hitches (figure 2*f*, electronic supplementary material, figure S2*b*,*d*–*g*) are consistent with previous findings that each wing receives information from both halteres, but that this information can be used to drive the wings independently. Flies are capable of apparently normal flight following unilateral haltere ablation [61]. In *Calliphora,* input from a single haltere is sufficient to entrain firing of the contralateral first basalare muscle following ablation of the ipsilateral haltere and both wing nerves [17]. Experiments rotating the fly's entire body showed that both amplitude and frequency components of haltere-wing reflexes are impaired following bilateral—but not unilateral—haltere ablation [19]. Similarly, manipulating the bulb mass of a single haltere produced comparable changes in both clockwise and counterclockwise body saccades [62].

This bilateral integration implicates the contralateral haltere interneurons, or cHINs [37,63], which receive input from haltere afferents and represent the only known anatomical pathway through which haltere information crosses the body axis. Though conserved across fly taxa, these neurons have eluded physiological characterization, leaving questions as to the sensory representations and transformations they mediate *en route* to their motor targets. One possibility is that the predominately unilateral hitches observed in our data might represent 'building blocks' that the thoracic nervous system can assemble into more complicated manoeuvres such as saccades that coordinate tightly across the body axis. This interpretation would accord with recent findings showing that a small population of descending neurons govern the initiation of saccades, recruiting elements of the flight control network via as-yet uncharacterized targets in each of the major thoracic neuromeres [64–66].

(c) Active attenuation of wing and gaze optomotor responses by halteres

Descending visual inputs target the same wing and gaze motoneurons as halteres, prompting investigation of multisensory control over these two motor systems [37,38,67]. Vision is susceptible to motion blur and requires significant signal transduction and processing time that constrains the stable operating range of systems under visual feedback control [55,68]. In flies, systems identification and control theory perspectives have shown a recurring motif in which high amplitude, visually initiated movements are actively damped by fast mechanosensory reflexes. Examples include damping of optical flow-based velocity control by antennae [69], as well as state-dependent damping of body orientation [21,50,55,62] and head posture [36] by halteres during visually guided manoeuvres.

Our findings are congruent with this framework showing that dynamic haltere stimulation severely attenuates the wing optomotor response and reduces the gain of the gaze optomotor response (figure 5). Mechanistically, these findings may reflect the role of the visual-haltere control loop, in which descending neurons provide excitatory input to haltere muscles and change the stroke parameters or mechanical properties of the haltere hinge during active turns [18,67,70]. This concomitantly changes the sensory input from the haltere [18,70], recruiting the haltere-wing and haltere-gaze reflex loops into the steering manoeuvre. Our experiment breaks this control loop by nullifying this relationship between haltere muscle activity and haltere sensory input; the treated haltere moves the same way regardless of any concurrent visual input, 'locking' its contributions to downstream motor systems to parameters induced by the stimulation. This could explain why visual input cannot 'rescue' the wing from high hitch rates (figure 4) and why visual tuning is ablated in the wings (figure 5*g*–*i*).

Compared with the wings, it is less clear how the head might respond to asynchronous haltere input. Recent work has shown that head movements follow a position-dependent control scheme [34], with activation of particular motoneurons capable of driving movements in different directions depending upon proprioceptive inputs from neck chordotonal organs [71]. Input from the halteres is necessary to adjust the gain of the head optomotor response to different pattern velocities [40], and self-generated body rotations are accompanied by larger amplitude head movements than imposed body rotations [36]. In some neck motoneurons of quiescent *Calliphora*, an absence of haltere input prevents spiking responses to visual input, but spiking can be restored with haltere movement at any frequency, even as low as 10 Hz [41]. If the halteres are necessary only to provide excitatory drive, then asynchronous input should produce gaze optomotor tuning curves with similar gain to an

untreated control. Instead, we found that asynchronous drive resulted in lower gain, and no loss in ability to tune the gain of the response to different pattern velocities (figure 5*i*). Future recordings of electrophysiological properties of neck motoneurons under different behavioural conditions and of haltere movement responses to visual inputs could help elucidate the role of halteres in this complex control logic.

Ethics. This work did not require ethical approval from a human subject or animal welfare committee.

Data accessibility. All processed data and associated videos are available in Dryad [72]. Kinematic time series for some untreated control animals in figures 1–5 are included with a previously published publicly available dataset [73].

Electronic supplementary material is available online at [74].

Declaration of AI use. We have not used AI-assisted technologies in creating this article.

Authors' contributions. M.J.R.: data curation, formal analysis, investigation, methodology, software, validation, visualization, writing—original draft, writing—review and editing; J.L.F.: conceptualization, funding acquisition, methodology, project administration, resources, supervision, writing—review and editing.

Both authors gave final approval for publication and agreed to be held accountable for the work performed therein.

Conflict of interest declaration. We declare we have no competing interests.

Funding. This work was supported by United States Air Force Office of Scientific Research [FA9550-14-0398 and FA9550-16-1-0165 to J.L.F.]; and National Science Foundation [1754412 to J.L.F.].

Acknowledgements. We would like to thank Chenxin Bi and Brandon Chun for help with data collection and annotation, as well as Noah DeFino, Jesse Fritz and Lauren Metz for fly care. We would also like to thank Hillel Chiel, Bradley Dickerson, Jeremiah Didion, Alexandra Gurgis, Nicholas Kathman, Kristianna Lea, Mark Willis, Gabriella Wolff and Alexandra Yarger for helpful commentary.

References

1. Heckscher ES *et al*. 2015 Even-skipped(+) interneurons are core components of a sensorimotor circuit that maintains left-right symmetric muscle contraction amplitude. *Neuron* **88**, 314–329, (doi:10.1016/j.neuron.2015.09.009)
2. Wiggin TD, Peck JH, Masino MA. 2014 Coordination of fictive motor activity in the larval zebrafish is generated by non-segmental mechanisms. *PLoS One* **9**, e109117. (doi:10.1371/journal.pone.0109117)
3. Wannier T, Bastiaanse C, Colombo G, Dietz V. 2001 Arm to leg coordination in humans during walking, creeping and swimming activities. *Exp. Brain Res*. **141**, 375–379. (doi:10.1007/s002210100875)
4. Dickinson MH, Muijres FT. 2016 The aerodynamics and control of free flight manoeuvres in *Drosophila*. *Phil. Trans. R. Soc. B* **371**, 20150388. (doi:10.1098/rstb.2015.0388)
5. Hiebert GW, Pearson KG. 1999 Contribution of sensory feedback to the generation of extensor activity during walking in the decerebrate cat. *J. Neurophysiol*. **81**, 758–770. (doi:10.1152/jn.1999.81.2.758)
6. Noah JA, Quimby L, Frazier SF, Zill SN. 2004 Walking on a "peg leg": extensor muscle activities and sensory feedback after distal leg denervation in cockroaches. *J. Comp. Physiol. A Neuroethol. Sens. Neural. Behav. Physiol*. **190**, 217–231. (doi:10.1007/s00359-003-0488-x)
7. Dickinson MH. 1990 Comparison of encoding properties of campaniform sensilla on the fly wing. *J. Exp. Biol*. **151**, 245–261. (doi:10.1242/jeb.151.1.245)
8. Pringle JWS. 1948 The gyroscopic mechanism of the halteres of diptera. *Phil. Trans. R. Soc. B* **233**, 347–384. (doi:10.1098/rstb.1948.0007)
9. Sun M, Wang J, Xiong Y, Sun M, Wang J, Xiong Y. 2007 Dynamic flight stability of hovering insects. *Acta Mech. Sin*. **23**, 231–246. (doi:10.1007/s10409-007-0068-3)
10. Derham W. 1714 Physico-theology: or, a demonstration of the being and attributes of God, from his works of creation. being the substance of XVI sermons preached in St. Mary le bow-church, London, at the Honble Mr. boyle's lectures, in the years 1711 and 1712. W. and J. Innys, London, 1714. See https://archive.org/details/physicotheologyo00derh.
11. Gnatzy W, Grünert U, Bender M. 1987 Campaniform sensilla of *Calliphora vicina* (Insecta, Diptera). Zoomorphology **106**, 312–319.
12. Agrawal S, Grimaldi D, Fox JL. 2017 Haltere morphology and campaniform sensilla arrangement across diptera. *Arthropod Struct. Dev.* **46**, 215–229. (doi:10.1016/j.asd.2017.01.005)
13. Fox JL, Daniel TL. 2008 A neural basis for gyroscopic force measurement in the halteres of Holorusia. *J. Comp. Physiol. A Neuroethol. Sens. Neural. Behav. Physiol*. **194**, 887–897. (doi:10.1007/s00359-008-0361-z)
14. Yarger AM, Fox JL. 2018 Single mechanosensory neurons encode lateral displacements using precise spike timing and thresholds. *Proc. R. Soc. B* **285**, 20181759. (doi:10.1098/rspb.2018.1759)
15. Hall JM, McLoughlin DP, Kathman ND, Yarger AM, Mureli S, Fox JL. 2015 Kinematic diversity suggests expanded roles for fly halteres. *Biol. Lett*. **11**, 20150845. (doi:10.1098/rsbl.2015.0845)
16. Deora T, Singh AK, Sane SP. 2015 Biomechanical basis of wing and haltere coordination in flies. *Proc. Natl. Acad. Sci. USA* **112**, 1481–1486. (doi:10.1073/pnas.1412279112)
17. Heide G. 1983 Neural mechanisms of flight control in Diptera. In *Biona-report 2* (ed. W Nachtigall), pp. 35–52. Stuttgart, New York: Gustav Fischer Verlag.
18. Dickerson BH, de Souza AM, Huda A, Dickinson MH. 2019 Flies regulate wing motion via active control of a dual-function gyroscope. *Curr. Biol*. **29**, 3517–3524.(doi:10.1016/j.cub.2019.08.065)
19. Dickinson MH. 1999 Haltere-mediated equilibrium reflexes of the fruit fly, *Drosophila melanogaster*. *Phil. Trans. R. Soc. B* **354**, 903–916. (doi:10.1098/rstb.1999.0442)
20. Mureli S, Fox JL. 2015 Haltere mechanosensory influence on tethered flight behavior in *Drosophila*. *J. Exp. Biol*. **218**, 2528–2537. (doi:10.1242/jeb.121863)
21. Bartussek J, Lehmann FO. 2016 Proprioceptive feedback determines visuomotor gain in *Drosophila*. *R. Soc. Open Sci*. **3**, 150562. (doi:10.1098/rsos.150562)
22. Fayyazuddin A, Dickinson MH. 1996 Haltere afferents provide direct, electrotonic input to a steering motor neuron in the blowfly, *Calliphora*. *J. Neurosci*. **16**, 5225–5232. (doi:10.1523/JNEUROSCI.16-16-05225.1996)
23. Fayyazuddin A, Dickinson MH. 1999 Convergent mechanosensory input structures the firing phase of a steering motor neuron in the blowfly, *Calliphora* . *J. Neurophysiol*. **82**, 1916–1926. (doi:10.1152/jn.1999.82.4.1916)
24. Rauscher MJ, Fox JL. 2021 Haltere and visual inputs sum linearly to predict wing (but not gaze) motor output in tethered flying *Drosophila*. *Proc. R. Soc. B* **288**, 20202374. (doi:10.1098/rspb.2020.2374)
25. Götz KG. 1979 The optomotor equilibrium of the Drosophila navigation system. *J. Comp. Physiol. A.* **99**, 187–210. (doi:10.1007/BF00613835)
26. Heisenberg M, Wolf R. 1984 Vision in *Drosophila*: genetics of microbehavior. In Studies of brain function (ed. V Braitenberg), p. 95. Berlin Heidelberg New York Tokyo: Springer.
27. Land MF, Collett TS. 1974 Chasing behaviour of houseflies (*Fannia canicularis*). *J. Comp. Physiol* **89**, 331–357. (doi:10.1007/BF00695351)

28. Land MF. 1973 Head movement of flies during visually guided flight. *Nature* **243**, 299–300. (doi:10.1038/243299a0)
29. Bender JA, Dickinson MH. 2006 Visual stimulation of saccades in magnetically tethered *Drosophila* . *J. Exp. Biol*. **209**, 3170–3182. (doi:10.1242/jeb.02369)
30. Mongeau JM, Frye MA. 2017 *Drosophila* spatiotemporally integrates visual signals to control saccades. *Curr. Biol*. **27**, 2901–2914.(doi:10.1016/j.cub.2017.08.035)
31. Kim AJ, Fitzgerald JK, Maimon G. 2015 Cellular evidence for efference copy in *Drosophila* visuomotor processing. *Nat. Neurosci*. **18**, 1247–1255. (doi:10.1038/nn.4083)
32. Kim AJ, Fenk LM, Lyu C, Maimon G, Otsuna H, Ito K, Borst A, Reiff DF. 2017 Quantitative predictions orchestrate visual signaling in Drosophila. *Curr. Biol.* **168**, 280–294. (doi:10.1016/j.cell.2016.12.005)
33. Schilstra C, van Hateren JH. 1998 Stabilizing gaze in flying blowflies. *Nature* **395**, 654. (doi:10.1038/27114)
34. Cellini B, Salem W, Mongeau JM. 2021 Mechanisms of punctuated vision in fly flight. *Curr. Biol*. **31**, 4009–4024.(doi:10.1016/j.cub.2021.06.080)
35. Cellini B, Mongeau JM. 2020 Active vision shapes and coordinates flight motor responses in flies. *Proc. Natl. Acad. Sci. USA* **117**, 23085–23095. (doi:10.1073/pnas.1920846117)
36. Cellini B, Mongeau JM. 2022 Nested mechanosensory feedback actively damps visually guided head movements in *Drosophila*. *eLife* **11**, e80880. (doi:10.7554/eLife.80880)
37. Strausfeld NJ, Seyan HS. 1985 Convergence of visual, haltere, and prosternai inputs at neck motor neurons of *Calliphora erythrocephala*. *Cell Tissue Res.* **240**, 601–615. (doi:10.1007/BF00216350)
38. Namiki S, Dickinson MH, Wong AM, Korff W, Card GM. 2018 The functional organization of descending sensory-motor pathways in *Drosophila*. *Elife* **7**, e34272. (doi:10.7554/eLife.34272)
39. Hengstenberg R, Sandeman DC, Hengstenberg B. 1986 Compensatory head roll in the blowfly Calliphora during flight. *Proc. R. Soc. B.* **227**, 455–482. (doi:10.1098/rspb.1986.0034)
40. Mureli S, Thanigaivelan I, Schaffer ML, Fox JL. 2017 Cross-modal influence of mechanosensory input on gaze responses to visual motion in *Drosophila*. *J. Exp. Biol*. **220**, 2218–2227. (doi:10.1242/jeb.146282)
41. Huston SJ, Krapp HG. 2009 Nonlinear integration of visual and haltere inputs in fly neck motor neurons. *J. Neurosci*. **29**, 13097–13105. (doi:10.1523/JNEUROSCI.2915-09.2009)
42. Reiser MB, Dickinson MH. 2008 A modular display system for insect behavioral neuroscience. *J. Neurosci. Methods* **167**, 127–139. (doi:10.1016/j.jneumeth.2007.07.019)
43. Fox JL, Aptekar JW, Zolotova NM, Shoemaker PA, Frye MA. 2014 Figure-ground discrimination behavior in *Drosophila*. I. spatial organization of wing-steering responses. *J. Exp. Biol*. **217**, 558–569. (doi:10.1242/jeb.097220)
44. Hedrick TL. 2008 Software techniques for two- and three-dimensional kinematic measurements of biological and biomimetic systems. *Bioinspir. Biomim.* **3**, 34001. (doi:10.1088/1748-3182/3/3/034001)
45. Mathis A, Mamidanna P, Cury KM, Abe T, Murthy VN, Mathis MW, Bethge M. 2018 DeepLabCut: markerless pose estimation of user-defined body parts with deep learning. *Nat. Neurosci*. **21**, 1281–1289. (doi:10.1038/s41593-018-0209-y)
46. Suver MP, Huda A, Iwasaki N, Safarik S, Dickinson MH. 2016 An array of descending visual interneurons encoding self-motion in *Drosophila*. *J. Neurosci*. **36**, 11768–11780. (doi:10.1523/JNEUROSCI.2277-16.2016)
47. Namiki S, Ros IG, Morrow C, Rowell WJ, Card GM, Korff W, Dickinson MH. 2022 A population of descending neurons that regulates the flight motor of *Drosophila*. *Curr. Biol*. **32**, 1189–1196.(doi:10.1016/j.cub.2022.01.008)
48. Duistermars BJ, Reiser MB, Zhu Y, Frye MA. 2007 Dynamic properties of large-field and small-field optomotor flight responses in *Drosophila*. *J. Comp. Physiol. A. Neuroethol. Sens. Neural. Behav. Physiol.* **193**, 787–799. (doi:10.1007/s00359-007-0233-y)
49. Schwyn DA, Heras FJH, Bolliger G, Parsons MM, Krapp HG, Tanaka RJ. 2011 Interplay between feedback and feedforward control in fly gaze stabilization. IFAC Proc. Vol. (IFAC-PapersOnline) **44**, 9674–9679. (doi:10.3182/20110828-6-IT-1002.03809)
50. Rimniceanu M, Currea JP, Frye MA. 2023 Proprioception gates visual object fixation in flying flies. *Curr. Biol*. **33**, 1459–1471.(doi:10.1016/j.cub.2023.03.018)
51. Zill SN, Moran DT. 1981 The exoskeleton and insect proprioception. I. Responses of tibial campaniform sensilla to external and muscle-generated forces in the American cockroach, *Periplaneta americana*. *J. Exp. Biol.* **91**, 1–24. (doi:10.1242/jeb.91.1.1)
52. Chapman KM, Smith RS. 1963 A Linear transfer function underlying impulse frequency modulation in a cockroach mechanoreceptor. *Nature* **197**, 699–700. (doi:10.1038/197699a0)
53. Nalbach G. 1993 The halteres of the blowfly *Calliphora*. *J. Comp. Physiol. A* **173**, 293–300. (doi:10.1007/BF00212693)
54. Haag J, Wertz A, Borst A. 2010 Central gating of fly optomotor response. *Proc. Natl Acad. Sci. USA* **107**, 20104–20109. (doi:10.1073/pnas.1009381107)
55. Elzinga MJ, Dickson WB, Dickinson MH. 2012 The influence of sensory delay on the yaw dynamics of a flapping insect. *R. Soc. Interface* **9**, 1685–1696. (doi:10.1098/rsif.2011.0699)
56. Sherman A, Dickinson MH. 2004 Summation of visual and mechanosensory feedback in *Drosophila* flight control. *J. Exp. Biol*. **207**, 133–142. (doi:10.1242/jeb.00731)
57. Lindsay T, Sustar A, Dickinson MH. 2017 The function and organization of the motor system controlling flight maneuvers in flies. *Curr. Biol*. **27**, 345–358, (doi:10.1016/j.cub.2016.12.018)
58. Heide G, Götz KG. 1996 Optomotor control of course and altitude in *Drosophila melanogaster* is correlated with distinct activities of at least three pairs of flight steering muscles. *J. Exp. Biol*. **199**, 1711–1726. (doi:10.1242/jeb.199.8.1711)
59. Tu MS, Dickinson MH. 1996 The control of wing kinematics by two steering muscles of the blowfly (*Calliphora vicina*). *J. Comp. Physiol. A.* **178**, 813–830. (doi:10.1007/BF00225830)
60. Balint CN, Dickinson MH. 2001 The correlation between wing kinematics and steering muscle activity in the blowfly *Calliphora vicina*. *J. Exp. Biol*. **204**, 4213–4226. (doi:10.1242/jeb.204.24.4213)
61. Fraenkel G. 1939 The function of the halteres of flies (*Diptera*). *Proc. Zoo. Soci. Lond.* **A109**, 69–78. (doi:10.1111/j.1096-3642.1939.tb00049.x)
62. Bender JA, Dickinson MH. 2006 A comparison of visual and haltere-mediated feedback in the control of body saccades in *Drosophila melanogaster*. *J. Exp. Biol*. **209**, 4597–4606. (doi:10.1242/jeb.02583)
63. Trimarchi JR, Murphey RK. 1997 The shaking-B2 mutation disrupts electrical synapses in a flight circuit in adult *Drosophila*. *J. Neurosci.* **17**, 4700–4710. (doi:10.1523/JNEUROSCI.17-12-04700.1997)
64. Schnell B, Ros IG, Dickinson MH. 2017 A descending neuron correlated with the rapid steering maneuvers of flying *Drosophila*. *Curr. Biol*. **27**, 1200–1205, (doi:10.1016/j.cub.2017.03.004)
65. Ferris BD, Green J, Maimon G. 2018 Abolishment of spontaneous flight turns in visually responsive *Drosophila*. *Curr. Biol*. **28**, 170–180.(doi:10.1016/j.cub.2017.12.008)
66. Ros IG, Omoto JJ, Dickinson MH. 2024 Descending control and regulation of spontaneous flight turns in *Drosophila*. *Curr. Biol*. **34**, 531–540.(doi:10.1016/j.cub.2023.12.047)
67. Chan WP, Prete F, Dickinson MH. 1998 Visual input to the efferent control system of a fly's "gyroscope." *Science* **280**, 289–292. (doi:10.1126/science.280.5361.289)
68. Hardcastle BJ, Krapp HG. 2016 Evolution of biological image stabilization. *Curr. Biol*. **26**, R1010–R1021, (doi:10.1016/j.cub.2016.08.059)
69. Fuller SB, Straw AD, Peek MY, Murray RM, Dickinson MH. 2014 Flying *Drosophila* stabilize their vision-based velocity controller by sensing wind with their antennae. *Proc. Natl. Acad. Sci. USA* **111**, E1182–91. (doi:10.1073/pnas.1323529111)
70. Verbe A, Lea KM, Fox JL, Dickerson BH. Flies tune the sensitivity of their multifunctional gyroscope. *bioRXiv*. (doi:10.1101/2024.03.13.583703)
71. Gorko B *et al*. 2024 Motor neurons generate pose-targeted movements via proprioceptive sculpting. *Nature* **628**, 596–603. (doi:10.1038/s41586-024-07222-5)

72. Rauscher M, Fox J. 2024 Data for: Asynchronous haltere input drives specific wing and head movements in *Drosophila*. Dryad Digital Repository (doi:.org/10.5061/dryad.g1jwstqwj)
73. Rauscher MJ, Fox JL. 2020 Data for: Weighted haltere and imposed haltere stroke reduction tethered flying *Drosophila* kinematics. Dryad Digital Repository (doi:10.5061/dryad.g4f4qrfnr)
74. Rauscher M, Fox JL. 2024 Supplementary material from: Asynchronous haltere input drives specific wing and head movements in *Drosophila*. Figshare (doi:10.6084/m9.figshare.c.7204039)